CORONARY ANGIOPLASTY AND GUIDEWIRE DIAGNOSTICS

Rupak K. Banerjee
Abhijit Sinha Roy
University of Cincinnati
Cincinnati, Ohio

Lloyd H. Back
California Institute of Technology
Pasadena, California

INTRODUCTION

Percutaneous transluminal coronary angioplasty (PTCA) is an invasive procedure, in which a blocked coronary artery is opened by inserting a pressurized balloon. Since its inception in the year 1964 (1), coronary angioplasty has undergone much development and is commonly performed in cardiac catheterization today. A statistic provided by the Centers for Disease Control (CDC) shows that nearly half a million PTCA procedures were conducted in the United States alone in the year 2002. A typical coronary angioplasty procedure includes these basic components, as follows.

Guiding Catheter

A guiding catheter serves three broad purposes (2):

1. Provides support and passage to the introduction of smaller diameter guidewires.
2. Provides a conduit to the administration of drugs and external agents such as contrast agent in angiography.
3. Provides damping, due to heart motion, to guidewires inserted through them.

For passage of guidewires, a catheter, having a diameter at least twice that of the guidewire, is recommended. Most guidewires are made up of soft material in the tip so that the amount of vessel injury is as minimal as possible. In modern practice, guiding catheters are available in different shapes, such as Judkins, Amplatz curves, pig tail, and sizes. Selection of a suitable guiding catheter depends on specific procedures. Small-sized guiding catheters of size 6F and 7F are most commonly used in PTCA as their size is well suited for guidewires of size 0.35 mm ($=$0.014 in.) and for passage of balloon catheters, compatible with coronary vessel dimensions of humans. Some guiding catheters may be designed with side holes at the end, which enables them to engage the coronary ostium, while maintaining continuous administration of fluoroscopy agent. The length of guiding catheters is around 90–100 cm. Figure 1 shows some guiding catheters being used today in coronary angioplasty.

Guidewires

Modern-day guidewires are designed for tip stiffness, easy maneuverability, location control, and visibility to angiography. A typical guidewire has a solid core, usually made up of stainless steel or nitinol and has a gradual taper from the proximal to distal end. This core is encapsulated in a spring coil and platinum in the distal section for improved radiographic visibility. The spring coil, which is a Teflon-coated stainless steel, is usually welded to directly or through a band to the tapered end of a guidewire so that the user may bend the tip to access the desired artery. Guidewires are available in a wide range of sizes from 0.25 mm ($=$0.010 in.) to 0.46 mm ($=$0.018 in.). In some cases, double length ($\sim$ 300 cm) guidewires may also be used, which enable access to the diseased vessel while other devices such as stent, dilation catheters are being deployed, with minimal risk of vessel injury (3).

Several specialized guidewires are also available. These guidewires are designed for measurement of arterial pressure and flow to assess the ischemic severity of a stenosis. For pressure measurement, a piezoelectric pressure transducer is placed around the inner solid core of the guidewire, around 3 cm from the tip (Fig. 2). This transducer facilitates measurement of transstenotic pressure drop and myocardial fractional flow reserve ($FFR_{myo\text{-}g}$) (4). These pressure sensors can measure pressure in the range of -30 to 300 mmHg with an accuracy of ± 1 mmHg. For phasic flow measurement, the technology most widely used is a Doppler-based flow sensor. The Doppler flow sensor is placed at the tip of the guidewire ($\sim$ 175 cm long). The ultrasound beam describes a conical region in the distal vessel, which thus obtains a small sample volume. The Doppler-based guidewire can measure translesional velocity, which is reported as coronary flow reserve (CFR $=$ coronary flow at hyperemia/coronary flow at basal flow). However, currently, Doppler guidewires are designed to measure average peak velocity, mean velocity for a cycle, as well as diastolic/systolic flow ratio. Another technique used to measure flow is based on coronary thermodilution. In this method, the wire has a microsensor at a location 3 cm from the floppy tip, which enables simultaneous recording of coronary pressure and temperature, with an accuracy of 0.02 °C (5,6). The shaft of this wire can be used as a second thermistor, which provides the input signal at the coronary ostium of any fluid injection at a temperature different from blood. CFR with this method is expressed as the ratio of mean transit time at basal flow to mean transit time at hyperemic flow. Experimentally, it has been shown that $CFR_{doppler}$and CFR_{thermo} differ by around 20% (5,6). To facilitate simultaneous evaluation of epicardial and microvascular diseases, a single wire, having both pressure and a Doppler flow sensor, has also been developed (7).

Balloon Catheter

Appropriate selection of a balloon catheter is a must for the success of coronary angioplasty. Beginning from the "over the wire" design, balloons have undergone many improvements. Current balloon catheters are both strong and flexible enough to handle a tortuous vessel segment, with

Encyclopedia of Medical Devices and Instrumentation, Second Edition, edited by John G. Webster

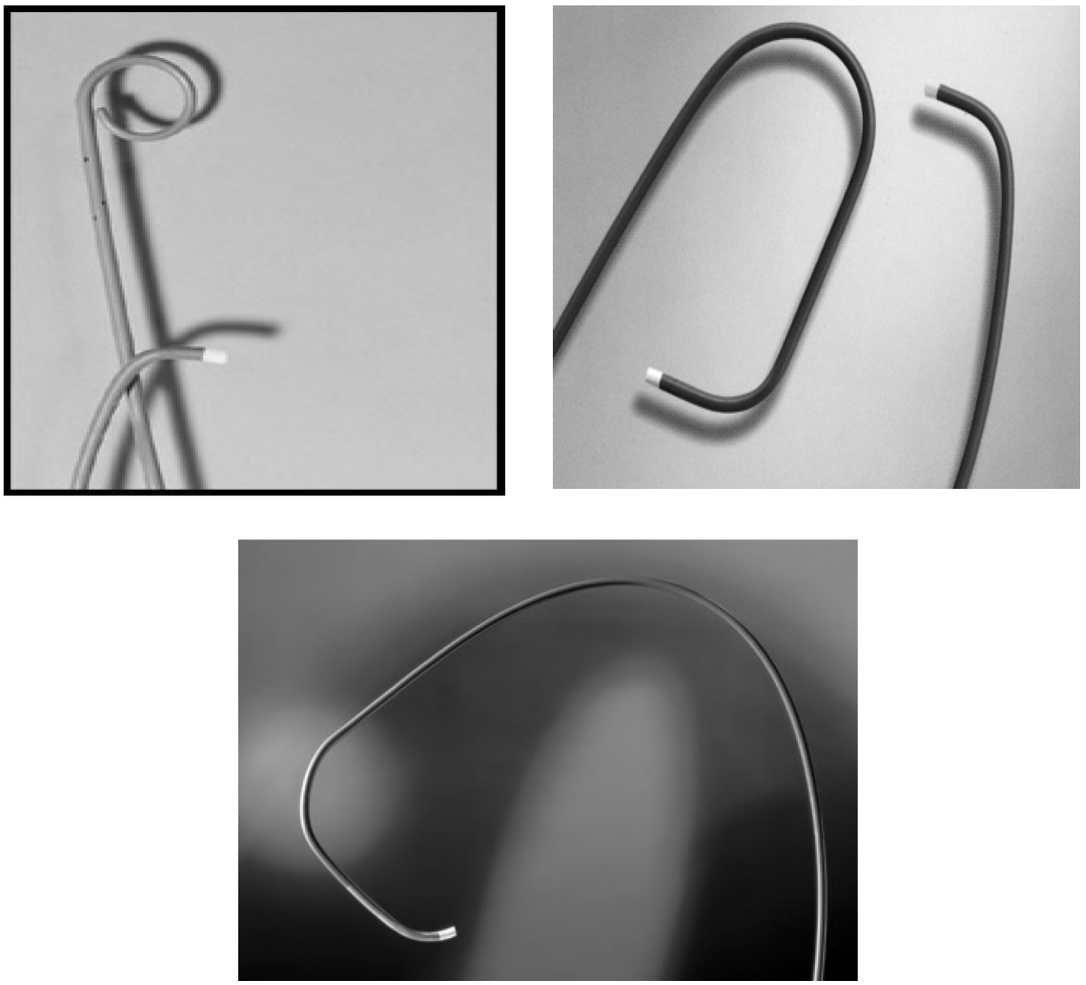

Figure 1. A few coronary angioplasty guiding catheters. Courtesy of Boston Scientific, MA.

minimal intimal injury. Most balloon catheters have a silicone or hydrophilic coating such as polyethylene to reduce friction. To dilate a balloon catheter, pressures up to 20 atm can be used. Figure 3a and b show a balloon catheter, having an "over the wire" design, with and without a stent. To generate the pressure, an indeflator is used. It consists of a cylinder, one end of which has a movable plunger and the other end is connected to the dilation catheter (Fig. 3c). The indeflator is partially filled with liquid and has an attached pressure gage. Dilation catheters have a wide range of inflation diameters ranging from 1.5 to 4 mm depending on the lumen dimension. Length of balloons varies from 10 mm to as much as 40 mm depending on the length of the atherosclerotic lesion. Materials used for manufacturing balloons can be polyethylene, polyolyfin, or nylon, to name some, with the wall thickness varying from 0.0003 in. to 0.0005 in. (2). Additionally, all balloon catheters are sold with a "rated burst pressure."

Besides the traditional design in which the catheter passes over the entire length of the guidewire, a design known as "monorail" is one in which the catheter passes just on its tip such that quick removal and insertion can be done. Some balloon catheters (perfusion balloons) are equipped with side holes at their tips in the shaft proximal and distal to the balloon to allow the blood to flow from the proximal to the distal vessel, when the balloon is inflated. It reduces the risk of ischemia in the heart (2). Nowadays, PTCA is usually combined with implantation of a stent in the clogged artery to keep the artery open, after balloon removal, and reduce the risk of restenosis. The path of approach of catheters and guidewires into the coronaries is usually done via the femoral artery and vein with direction guidance being provided by fluoroscopy. Other paths of approarch can be done via the axillary, brachial, or radial artery. For insertion of balloon as well as normal catheters and guidewires, percutaneous needles, such as the seldinger needle for the femoral artery and the Potts–Cournand

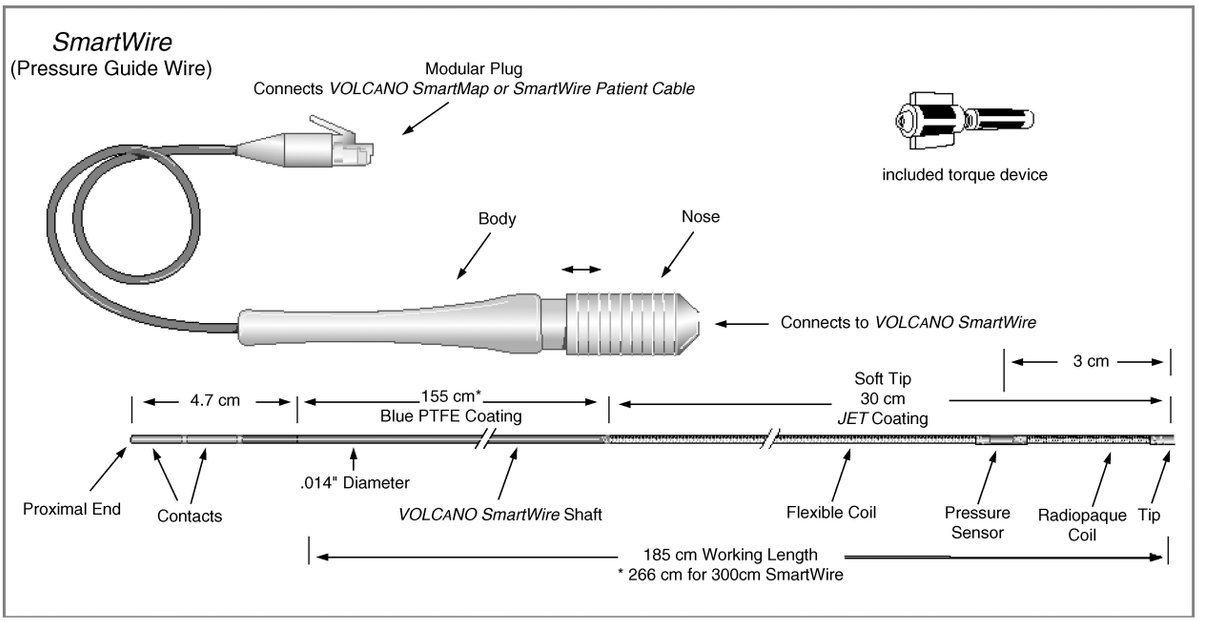

A guidewire for measuring pressure.

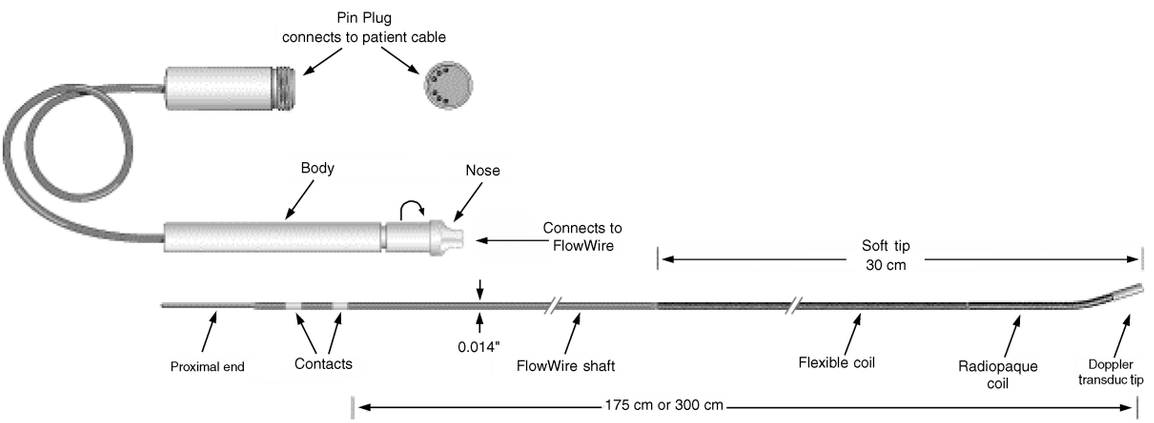

A guidewire for measuring flow.

Figure 2. Guidewires for measuring pressure and flow in diseased coronary arteries. Courtesy of Volcano Therapeutics Inc., CA.

needle (which is hollow from inside so that the user can know when the artery has been punctured), and vascular sheaths are also used. In case there is difficulty in detecting the arterial or venous pulse, a smart needle (PSG, Mountain View, CA) may be used, which has a Doppler crystal to direct the needle to the center of the vessel while sensing blood flow (2).

Vessel Closure Devices

On completion of PTCA, the punctured vessel needs to be closed to prevent any postprocedural bleeding followed by coagulation. The most commonly used device is a collagen plug applied to skin outside the outer wall of the vessel (8). Another device, called the Hemostatic Puncture Closure Device, also known as the Angio-Seal Vascular Closure device (St. Jude Medical Inc., St. Paul, MN; "Angio-Seal" is a registered trademark) uses an anchor on the inner wall of the vessel and an attached suture to raise a collagen plug to the outer wall of the vessel (9). Figure 4 shows the procedure followed to close the vessel using the Angio-Seal device. Another device, called the Prostar device (Perclose, Redwood City, CA), uses a sheath-like device to pass a suture around the puncture through the skin to close the puncture.

DIAGNOSTICS WITH GUIDEWIRES

With widespread use of PTCA, there has been a surge in the use of guidewires for evaluation of ischemic severity of focal and diffuse lesions before and after angioplasty. Since their inception, several authors (e.g., Refs. 10–13) have validated the usefulness of catheters and guidewires in

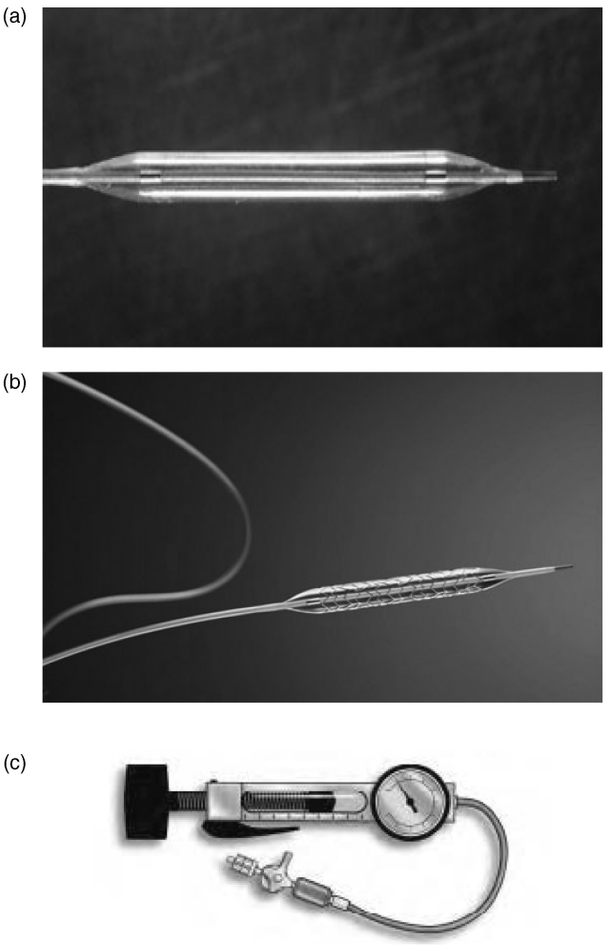

Figure 3. (a) An example of coronary dilation catheter; (b) with stent over it. This is an "over the wire design." Courtesy of Boston Scientific, MA.; (c) An indeflator, which is used to inflate the balloon. Courtesy of Guidant Corp., IN.

clinical procures, including PTCA. However, during coronary intervention, the introduction of guidewire produces an additional resistance to blood flow that has not been well documented.

Issues

The current usage of guidewires for coronary stenoses diagnostics is for measurement of myocardial fractional flow reserve ($FFR_{myo\text{-}g}$) and coronary flow reserve (CFR_g). The concept of coronary flow reserve was first introduced and applied by Gould et al. (14–16) to evaluate the functional severity of a coronary stenosis. CFR_g is the ratio of mean coronary flow at hyperemia ($\tilde{Q}_{h-g}$) to mean coronary flow at basal, i.e., rest ($\tilde{Q}_b$). Thus, to obtain CFR_g, blood flow is measured first at basal condition ($\tilde{Q}_b$). Then, after administration of a vasodilator agent, the blood flow is enhanced and measured. The ratio between the latter and the former blood flow measured with guidwire provides CFR_g. Pulsed Doppler catheters and currently guidewires have been used in patients to measure changes in coronary

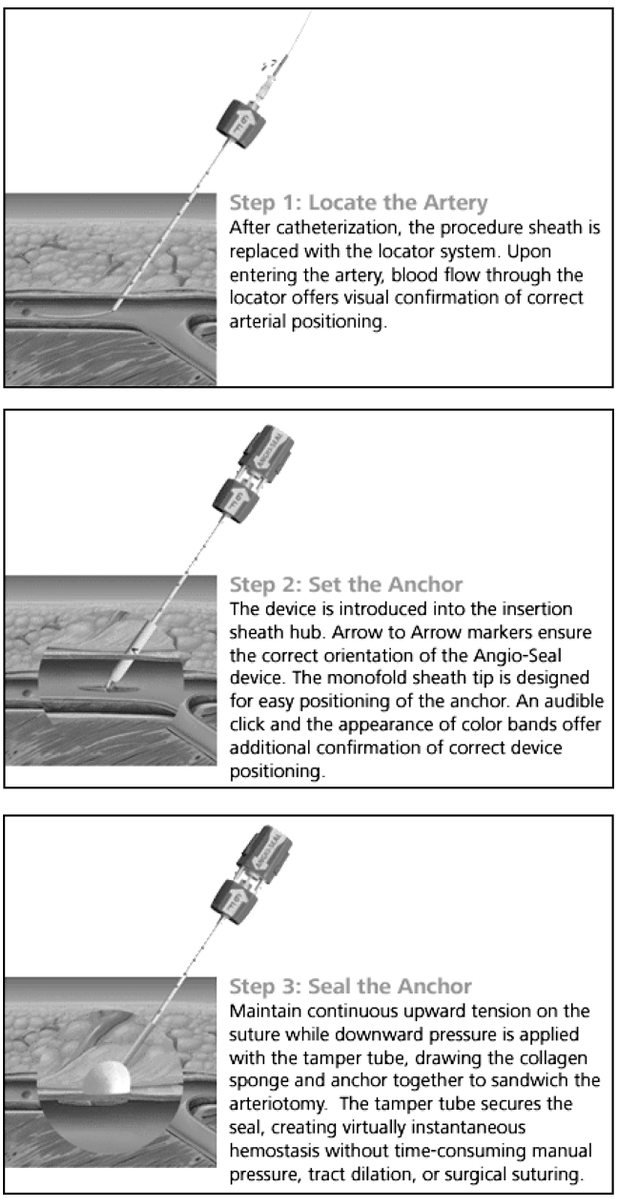

Figure 4. Vascular closure device, known as Angio-Seal. Courtesy of Kensey Nash., PA.

artery velocity in response to infusion of vasodilator agents (e.g., papaverine or adenosine) and to estimate CFR_g before and after clinical intervention of stenotic lesions. Thus, after PTCA, CFR_g increases due to an increase in flow area and a decrease in flow resistance to blood flow. However, the magnitude of increase is affected by the presence of microvascular disease, and flow disturbance distal to a stenosis hinders accurate measurement of CFR_g. Thus, CFR_g does not have any specific cutoff values for a normal and diseased coronary vessel with and without microvascular disease (17). Another flow limiting parameter, known as relative coronary flow reserve, $rCFR_g$ (14,18) was proposed. However, in patients in whom a stenotic artery supplies an area of myocardial infarction, neither CFR_g

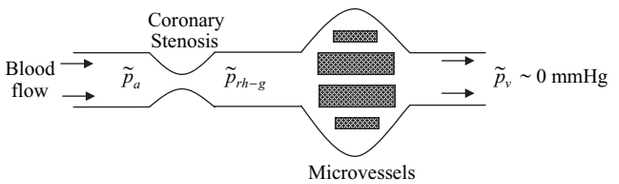

Figure 5. Measurement of myocardial fractional flow reserve in a coronary stenosis.

nor $rCFR_g$ can differentiate flow impairment due solely to a stenosis.

Introducing the latest technique of $FFR_{myo\text{-}g}$ measurement (4,17,19), it was shown that the hyperemic absolute distal coronary pressure ($\tilde{p}_{rh-g}$) is related to the ischemic potential of a stenosis, whereas the resting pressure is not. $FFR_{myo\text{-}g}$ is considered to be independent of driving pressure, heart rate, systemic blood pressure, and the status of the microcirculation; in addition, it reflects both antigrade and collateral coronary blood flow. By definition (4,17,19), $FFR_{myo\text{-}g}$ is the ratio of mean distal pressure ($\tilde{p}_{rh-g}$) to mean pressure proximal to the stenosis ($\tilde{p}_a$) at hyperemia, which is induced by administration of vasodilator agents, e.g., adenosine. As pressure drop in normal epicardial vessels is very small, $\tilde{p}_a$ is taken as mean aortic pressure. Thus, $FFR_{myo\text{-}g} = \frac{\tilde{p}_{rh-g} - \tilde{p}_v}{\tilde{p}_a - \tilde{p}_v}$, where $\tilde{p}_v =$ central venous pressure (Fig. 5). In human coronary circulation, $\tilde{p}_v$ is very low and close to zero. Therefore, to obtain $FFR_{myo\text{-}g}$, $\tilde{p}_v$ is assumed to be 0 mmHg (Fig. 5). Thus, if there is no coronary stenosis, $\tilde{p}_{rh-g} \cong \tilde{p}_a$ and $FFR_{myo\text{-}g} \sim 1$. Across a coronary stenosis, there will be a mean pressure drop ($\Delta\tilde{p}_{h-g}$). Thus, for a diseased coronary vessel, $\tilde{p}_{rh-g} < \tilde{p}_a$ and $FFR_{myo\text{-}g} < 1$. A value of $FFR_{myo\text{-}g} = 0.75$ is assumed to accurately discriminate stenosis whether or not it is associated with inducible ischemia (4,17,19). Both $FFR_{myo\text{-}g}$and CFR_g increase after coronary angioplasty, which thereby signifies an enhanced and normal blood supply to distal myocardium. However, simultaneous measurement of $FFR_{myo\text{-}g}$and CFR_g is recommended to dissociate an epicardial coronary lesion from distal microvascular disease (20,21).

Currently, guidewires of size 0.35 mm (=0.014 in.) can measure both flow (CFR_g) and mean pressure drop $\Delta\tilde{p}_{h-g}$ (and $FFR_{myo\text{-}g}$) across a stenosis. However, the introduction of a guidewire causes an obstructive effect, which creates an "artifactual" stenosis (22–25). The threshold limit of $FFR_{myo\text{-}g} = 0.75$ is a measured value with guidewire. However, this measured value of 0.75 must be attributed to $FFR_{myo\text{-}g}$ and not FFR_{myo}, the value for the lesion without guidewire obstruction. Limited information is available on what degree of flow blockage exists with currently used guidewires, although clinical investigators have acknowledged the limitations of mean pressure drop and flow measurements because of flow obstruction produced by guidewires (26). In the following sections, the authors present a summary of their past studies on guidewire diagnostics: (a) quantifying the flow obstruction effect of guidewires of diameter 0.35 mm (0.014 in.) and 0.46 mm (0.018 in.), which results in enhanced $\Delta\tilde{p}_h$ and reduced $\tilde{Q}_h$ in a significant, intermediate and moderate focal stenoses; and (b) corrections to be applied to $FFR_{myo\text{-}g}$and CFR_g to get true values of $FFR_{myo}$and CFR without guidewire, which thus improves the diagnosis of focal coronary lesions.

To evaluate the flow obstruction effect, stenoses geometry of a focal pre-PTCA (27,28) and post-PTCA lesion (29,30) were obtained from the *in vivo* data of a 32 patient group (31). The patients had single-vessel, single-lesion coronary artery disease with unstable or stable angina pectoris. Dimensions and shape of the coronary stenosis before and after angioplasty were obtained from quantitative biplanar X-ray angiography. Biplane angiography of each lesion in orthogonal projections (60° left anterior oblique and 30° right anterior oblique) resolved vessel widths with the cross-sectional area calculated from the equation for an ellipse, which were converted to mean diameters (Table 1, Fig. 6a). Patients with abnormalities that might affect the vasodilator capacity of the arteriolar vasculature were excluded from the study (31). Measured values of CFR with a 3F pulsed Doppler ultrasound catheter ($d_i = 1.0$ mm) with tip positioned proximal to the lesions (with minimal flow blockage) increased from 2.3 ± 0.1 to 3.6 ± 0.3 in the procedure; mean arterial pressure, measured in the coronary ostium, decreased from 89 ± 3 to 84 ± 3 mmHg as shown in Table 1 (31). In the flow analysis, the residual composite lesion was assumed to have a smooth, rigid plaque wall and round concentric shape. Additional dimensional data on the shape of similar size lesion were obtained from a past study on focal lesions (32).

Additionally, an intermediate stenosis (33) having maximal area blockage based on minimal diameter = 80% was used in this study (the dimensions of which are given in Fig. 6a) to include a wide range of lesion sizes for obtaining the correlations. However, this intermediate lesion size was not measured in the 32 patient group (31). Furthermore, for guidewire analyses, the guidewire was placed concentrically within the lesion (Fig. 7a–c). The concentric configuration of the guidewire within the lesion may give the largest pressure drop (22).

Table 1. Lesion Geometry and Hemodynamics Before, Intermediate, and After PTCA

Lesion	A_m, mm^2	d_m, mm	% Area Stenosis	l_m, mm	CFR	$\tilde{p}_a$ mmHg	$\Delta\tilde{p}_h$ mmHg	$\tilde{p}_{rh}$ mmHg	FFR_{myo}
Before-PTCA	0.7 ± 0.1	0.95	90	0.75	2.3 ± 0.1	89 ± 3	34	55	0.62
Intermediate	1.43	1.35	80	0.75	3.3	86	14.3	70.4	0.82
After-PTCA	2.5 ± 0.1	1.80	64	3	3.6 ± 0.3	84 ± 3	7.4	75.2	0.89

A_m, d_m, and l_m are the area, diameter, and length of the narrowest region of the stenoses; $\tilde{p}_a$ and $\tilde{p}_{rh}$ are the mean arterial pressure in the coronary ostium and distal to the stenosis under hyperemia; and $\Delta\tilde{p}_h$ is the hyperemic pressure drop across the stenosis.

(a)

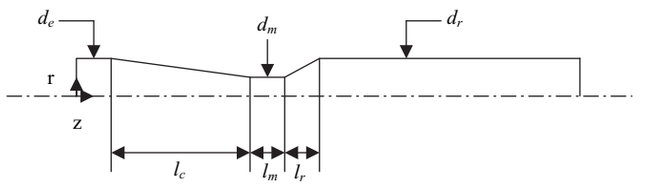

All dimensions in mm

	d_e	d_r	d_m	l_c	l_m	l_r	% Area Stenosis
Post-Angioplasty	3	3	1.8	6	3	1.5	64
Intermediate	3	3	1.35	6	0.75	1.5	80
Pre-Angioplasty	3	3	0.95	6	0.75	1.5	90

(b)

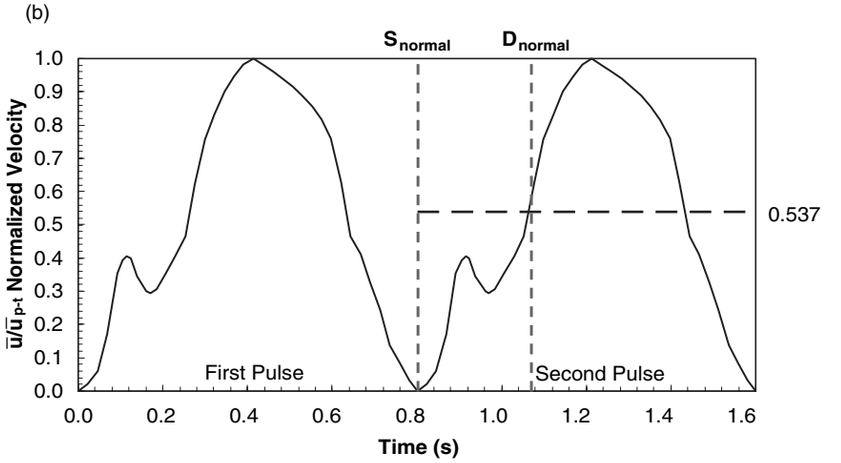

Figure 6. (a) Stenoses geometry shows the shape and dimensions in millimeters. (b) Normal coronary flow waveform $\bar{u}/\bar{u}_{p-t}$ vs. t, where S_{normal} indicates the beginning of systole and D_{normal} indicates the beginning of diastole.

(a)

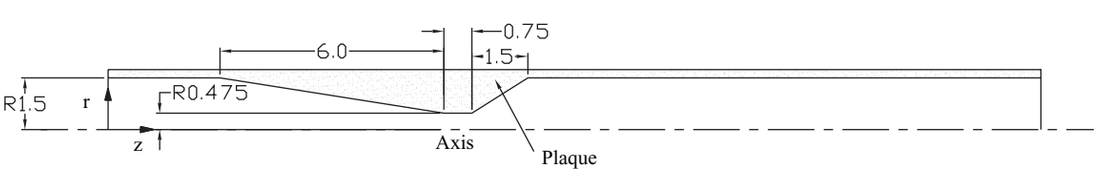

(i) Physiological Pre-PTCA

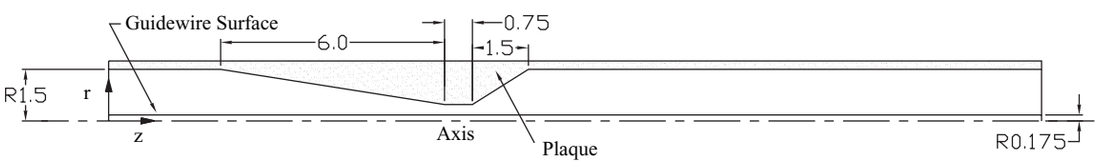

(ii) Pre-PTCA with 0.35 mm gw

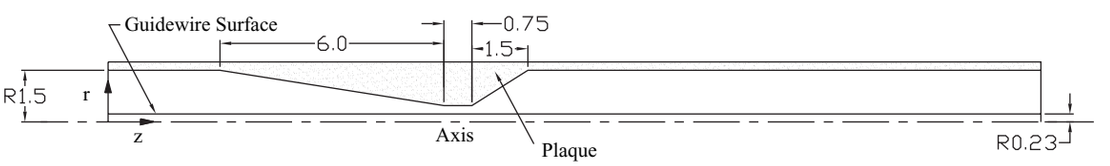

(iii) Pre-PTCA with 0.46 mm gw

Figure 7(a). (i) Pre-PTCA without guidewire. (ii) Pre-PTCA with 0.35 mm guidewire. (iii) Pre-PTCA with 0.46 mm guidewire.

The coronary velocity waveform $\overline{u}(t)$ (spatially averaged at each time across the cross-sectional area) used in the flow analyses was obtained in our laboratory from *in vitro* calibration (34), smoothing the fluctuating Doppler signal, and phase shifting the normal pattern for the proximal left anterior descending (LAD) artery. In Fig. 6b, the peak diastolic velocity $\overline{u}_{p-t}$ corresponds to a normalized velocity of 1.0, so that the ratio of mean to peak velocity $\widetilde{\overline{u}}/\overline{u}_{p-t}$ is 0.537 as shown by the dashed line.

With guidewire inserted concentrically, in the proximal vessel, the spatial velocity profile in the annular gap was taken to be the analogous Poiseuille flow relation for the axial velocity u (27,30):

$$u/2\overline{u} = [(1-(r/r_o)^2)\ln(r_o/r_i) + (1-(r_i/r_o)^2)\ln(r/r_o)]/ [(1+(r_i/r_o)^2)\ln(r_o/r_i) - (1-(r_i/r_o)^2)] \quad (1)$$

where u is a function of r and t and $r_o = r_e$. Without the guidewire, in the proximal vessel, the spatial velocity profile was initially taken to be the Poiseuille flow relation for the axial velocity u (28,29):

$$u/2\overline{u} = (1-(r/r_o)^2) \quad (2)$$

The Carreau model, which is given in equation 3, was used for shear-rate-dependent non-Newtonian blood viscosity with the local shear rate (equation 4) calculated from the velocity gradient through the second invariant of the rate of strain tensor (35).

$$\eta = \eta_\infty + (\eta_o - \eta_\infty)[1 + (\lambda\dot{\gamma})^2]^{(n-1)/2} \quad (3)$$

$$\dot{\gamma} = \sqrt{\frac{1}{2}\left[\sum_i \sum_j \dot{\gamma}_{ij}\dot{\gamma}_{ji}\right]} \quad (4)$$

where $\eta_\infty = 0.00345\,\text{Pa.s}$, $\eta_o = 0.056\,\text{Pa.s}$, $\lambda = 3.313\,\text{s}$, and $n = 0.3568$.

The details of the numerical method used to calculate the pulsatile hemodynamics in coronary artery and lesions with and without guidewire have been discussed in detail in past publications by the authors. A typical basal physiological value $\tilde{Q}_b = 50\,\text{ml/min}$ for a coronary vessel of 3-mm size was used (36). The cycle time of 0.8 s and density of blood $\rho = 1.05\,\text{gm/cm}^3$ was used. In the Reynolds number ($\tilde{\text{Re}}$), a kinematic viscosity of $\upsilon = 0.035\ \text{cm}^2/\text{s}$ was used, a value near the asymptote in the Carreau model for blood ($\eta_\infty \to 0.00345\,\text{Pa.s}$ as $\dot{\gamma} \to \infty$), which gives $\upsilon_\infty \to 0.033\,\text{cm}^2/\text{s}$. $\tilde{\text{Re}}$ for the complete range of flows from basal to hyperemic for the three stenoses varied from 100 to 360. The Womersley number (37), which is defined as $(r_e - r_i) \times \sqrt{\omega/\upsilon}$, varied from 1.98 with guidewire size 0.35 mm to 2.25 in the patho-physiological scenario without guidewire, i.e., $r_i = 0$.

CFR and $\tilde{p}_{rh}$ without guidewire and computed values of CFR_g and $\tilde{p}_{rh-g}$ for the different lesions with guidewire (0.35 and 0.46 mm) were used to construct the maximal vasodilation-distal perfusion pressure curve, which is also known as the $CFR - \tilde{p}_{rh}$ relationship (27–31,33). The maximal $CFR - \tilde{p}_{rh}$ curve was plotted by joining the measured and computed values of CFR and $\tilde{p}_{rh}$ at hyperemia for the native, intermediate, and residual lesions after angioplasty because blood was supplied to the same distal vasculature, which was originally with marked arteriolar dilation. The $CFR - \tilde{p}_{rh}$ relationship was then used to construct the correlations between FFR_myo and $\text{FFR}_\text{myo-g}$ and CFR and CFR_g in native, intermediate, and residual lesions for the two guidewires. The linear $CFR - \tilde{p}_{rh}$ was also extrapolated toward its origin to estimate zero-coronary flow mean pressure ($\tilde{p}_{z\,f}$) for the 32 patient group (31).

Diagnostics with Angioplasty Catheters

As an initial step, the authors calculated the $\Delta\tilde{p} - \tilde{Q}$ relationship post-PTCA (Curve J in Fig. 8), in conjunction with the pressure measurements, using the angioplasty catheter ($d_i = 1.4$ mm) before the development of small guidewire sensors (38). For resting conditions with the catheter present, flow was believed to be about 40% of normal basal flow in the absence of the catheter, and for hyperemia, about 20% of elevated flow in the patient group. Also, $\Delta\tilde{p}$ was significantly elevated in the tighter artifactual stenoses during the measurements. These diagnostic measurements were compared with the patho-physiologic scenario, having no angioplasty catheter. The results of patho-physiologic conditions cannot be measured in lesions, and they are descriptive of the unperturbed conditions that may have existed on average in the patient group after PTCA. In the absence of angioplasty catheter, the calculated $\Delta\tilde{p}$ was only ~1 mmHg at basal flow and increased moderately to ~7.4 mmHg for hyperemic flow measured proximally (CFR = 3.6) with minimal blockage. On the other hand, with the catheter, $\Delta\tilde{p}$ was ~28.7 mmHg for the basal flow showing an order of magnitude increase in $\Delta\tilde{p}$.

Increased pressure drop and reduced hyperemic flow due to the presence of guidewire

Tables 1 and 2 give the mean pressure drop $\Delta\tilde{p}_h$ and distal mean pressure $\tilde{p}_{rh}$ at hyperemic condition in native, intermediate, and residual lesions with and without guidewire (33). The ratio of guidewire diameter d_i to throat diameter d_m for different stenoses is given in Table 2. Guidewires of size 0.35 mm and 0.46 mm caused 30% to 45% overestimation in $\Delta\tilde{p}_h$ in the three stenoses as hyperemic flow was reduced by 5% to 37% from the physiologic condition without guidewire obstruction. Although diagnosis of severely blocked arteries is relatively easier and additional pressure drop due to the guidewire does not affect the diagnosis that much, it can be observed that additional pressure drop due to the guidewire could have an important role in clinical evaluation of moderate and intermediate stenoses. Furthermore, it can be observed that with guidewire of size 0.35 mm and 0.46 mm, $\text{FFR}_\text{myo-g} < \text{FFR}_\text{myo}$ and $\text{CFR}_\text{g} < \text{CFR}$ at hyperemia. The maximum decrease was observed in the native stenoses. The residual stenoses, i.e., post-PTCA, showed the least decrease. In summary, Fig. 8 shows the mean pressure drop from basal to hyperemic for the three stenoses with and without 0.35-mm and 0.46-mm guidewire.

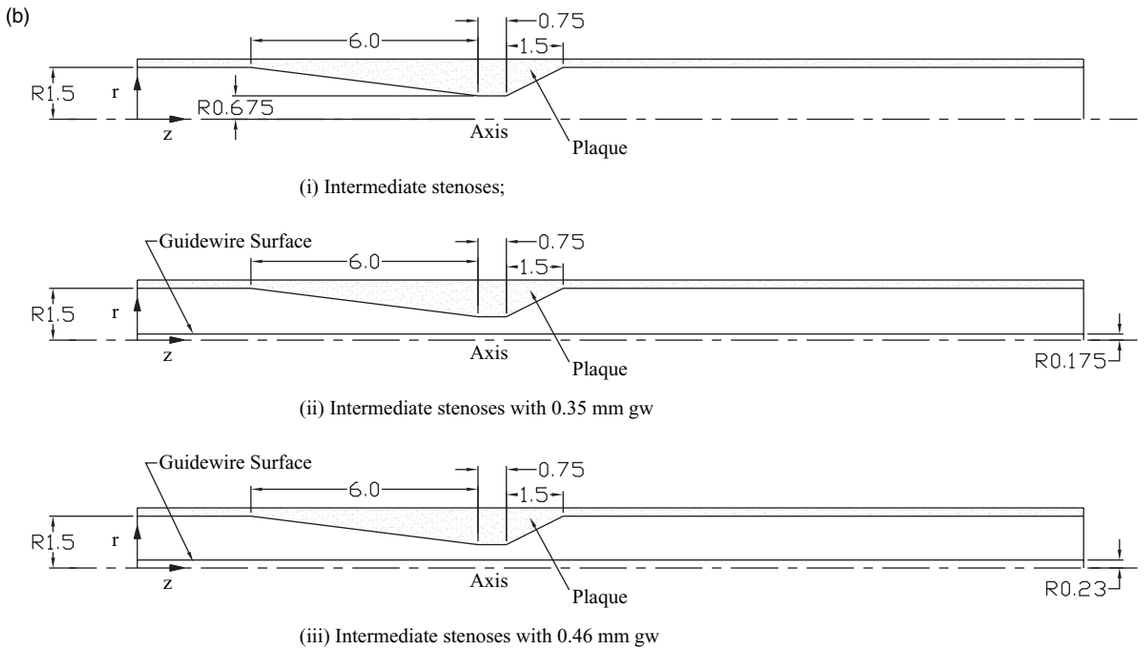

Figure 7(b). (i) Intermediate stenosis without guidewire. (ii) Intermediate stenosis with 0.35 mm guidewire. (iii) Intermediate stenosis with 0.46 mm guidewire.

Figure 9 shows the maximal $CFR - \tilde{p}_{rh}$ for the native, intermediate, and residual lesions after angioplasty with and without guidewire (33). Distal mean perfusion pressure for hyperemic flow $\tilde{p}_{rh}$ increased from 55 mmHg in pre-PTCA without guidewire to about 75 mmHg in post-PTCA without guidewire. $\tilde{p}_{rh}$ of 55 mmHg is indicative of subendocardium ischemia (39). Extrapolation of the nearly linear $CFR - \tilde{p}_{rh}$ relation toward its origin gave a zero-

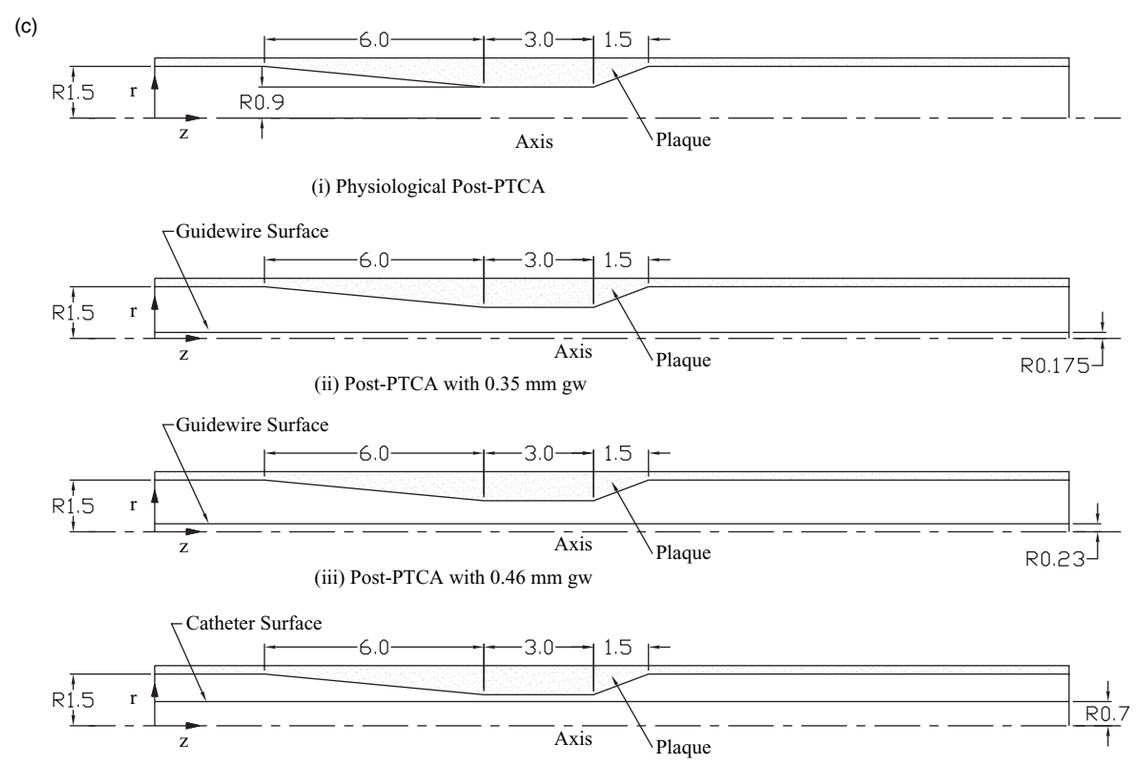

Figure 7(c). (i) Post-PTCA without guidewire. (ii) Post-PTCA with 0.35 mm guidewire. (iii) Post-PTCA with 0.46 mm guidewire. (iv) Post-PTCA with large angioplasty catheter.

Table 2. Hyperemic Mean Pressure Gradients and Distal Mean Pressure Before, Intermediate, and After Intervention with Guidewire

Lesion	$\tilde{p}_a$ mmHg	Guidewire size $d_i = 0.35$ mm $\frac{d_i}{d_m}$	$\tilde{Q}_{h-g}$ mL/min	$\Delta\tilde{p}_{h-g}$ mmHg	$\tilde{p}_{rh-g}$ mmHg	Guidewire size $d_i = 0.46$ mm $\frac{d_i}{d_m}$	$\tilde{Q}_{h-g}$ mL/min	$\Delta\tilde{p}_{h-g}$ mmHg	$\tilde{p}_{rh-g}$ mmHg
Before-PTCA	89	0.37	86.0	43.0	46.0	0.48	75.0	46.0	43.0
Intermediate	86	0.26	149.7	18.9	65.8	0.34	145.6	20.2	64.5
After-PTCA	84	0.19	172.5	9.9	72.8	0.26	170.0	10.6	72.1

Values obtained from the linear CFR- $\tilde{p}_{rh}$ curve.

coronary flow mean pressure ($\tilde{p}_{zf}$) of about 20 mmHg. This value is near a measured value of 18 mmHg (40), where myocardial blood flow ceased in the subendocardium layer of dog hearts, which were maximally dilated by infusion of adenosine.

FFR_{myo}-$FFR_{myo\text{-}g}$ and CFR-CFR_g Correlations

Table 3 provides the values of CFR, CFR_g, FFR_{myo}, and $FFR_{myo\text{-}g}$ for the different stenosis configurations (33). Figures 10 and 11 show the correlation plots between CFR and CFR_g and between FFR and FFR_g with their *linear* regression lines. In Fig. 10, **CFR** was related to $\mathbf{CFR_g}$ by the equation: with **guidewire size 0.46 mm**, $\mathbf{CFR = CFR_g \times\ 0.689 + 1.271\ (R^2 = 0.99)}$, and with **guidewire size 0.35 mm,** $\mathbf{CFR = CFR_g \times\ 0.757 + 1.004\ (R^2 = 0.99)}$. With central venous pressure ($\tilde{p}_v$) ~ 0, as used in current clinical practice, $\mathbf{FFR_{myo}}$ and $\mathbf{FFR_{myo\text{-}g}}$ correlated equally well (Fig. 11): with **guidewire size 0.46 mm,** $\mathbf{FFR_{myo} = FFR_{myo\text{-}g} \times\ 0.737 + 0.263\ (R^2 = 0.99)}$, and with **guidewire size 0.35 mm**, $\mathbf{FFR_{myo} = FFR_{myo\text{-}g} \times\ 0.790 + 0.210\ (R^2 = 0.99)}$, which gave $\mathbf{FFR_{myo} = 0.8}$ for a measured $\mathbf{FFR_{myo\text{-}g} = 0.75}$. The study showed that the correlations for guidewire size 0.35 mm are closer to the ideal (expected) relationship, i.e., $CFR = CFR_g$ and $FFR = FFR_g$ due to a relatively lesser flow obstruction effect than guidewire size 0.46 mm.

Usefulness of $FFR_{myo\text{-}g}$-FFR_{myo} and CFR-CFR_g Correlations

Although there are uncertainties associated with measurements of CFR with guidewires in diagnostic procedures as these measurements are made distal to the stenosis, these correlations could be useful in estimation of CFR and FFR_{myo} simultaneously from CFR_g and $FFR_{myo\text{-}g}$. It could provide useful information about the status of both the epicardial stenosis and the distal microcirculation during the procedure. As a result, CFR measurement proximal to the stenosis will be more accurate as this is the region of more stable flow. Furthermore, the heterogeneity of stenoses could produce variations in the slope of the correlations. However, the correlations were obtained based on stenosis shape and size measured invasively in a group of patients, and they have shown a direct and stronger relation to the minimal stenosis area as compared with the overall length and shape of the stenosis. Further clinical evaluation with a larger patient group will be needed to confirm the dominant effect of minimal stenosis area on these correlations.

Although several studies have focused on the relationship between CFR measured with guidewire and CFR measured with a noninvasive flow probe, e.g., Doppler cuff in animal studies, no similar study has been done to distinguish the effect of guidewire on FFR_{myo} as pressure can be measured invasively using guidewires only. Earlier *in vitro* measured Δp data (41) for steady flow of a saline solution through various blunt hollow plug stenosis models (50% to 90% area stenosis; $d_e = d_r = 4$ mm; $l_m = 10$ mm) with and without a small guidewire pressure sensor ($d_i = 0.38$ mm) also indicated appreciable overestimation of the true Δp as the severity of stenoses increased. In particular, for a 90% area stenosis ($[d_i/d_m] = 0.30$) at a flow rate $Q = 120$ mL/min, the mean pressure drop increased from 16 mmHg to 23 mmHg, which is ~40% increase, due to the increased flow resistance with the guidewire spanning the model stenosis in the rigid plastic tube having $d_e = 4$ mm. This detailed hemodynamic analysis in a smaller coronary vessel ($d_e = 3$ mm; 90% area stenosis; larger

Table 3. Effect of the Presence of Guidewire on the Values of CFR and FFR_{myo} at Hyperemic Conditions in Comparison with Values of CFR and FFR_{myo} under Patho-physiological Condition for Different Guidewire Sizes $d_i = 0.35$ mm (0.014 in.) and 0.46 mm (0.018 in.)

Lesion	Physiological CFR	Physiological FFR_{myo} With $\tilde{p}_v \sim 0$	0.35-mm Guidewire CFR_g	0.35-mm Guidewire $FFR_{myo\text{-}g}$ With $\tilde{p}_v \sim 0$	0.46-mm Guidewire CFR_g	0.46-mm Guidewire $FFR_{myo\text{-}g}$ With $\tilde{p}_v \sim 0$
Before-PTCA	2.3	0.62	1.72	0.52	1.50	0.48
Intermediate	3.3	0.82	2.99	0.76	2.91	0.75
After-PTCA	3.6	0.89	3.45	0.87	3.40	0.86

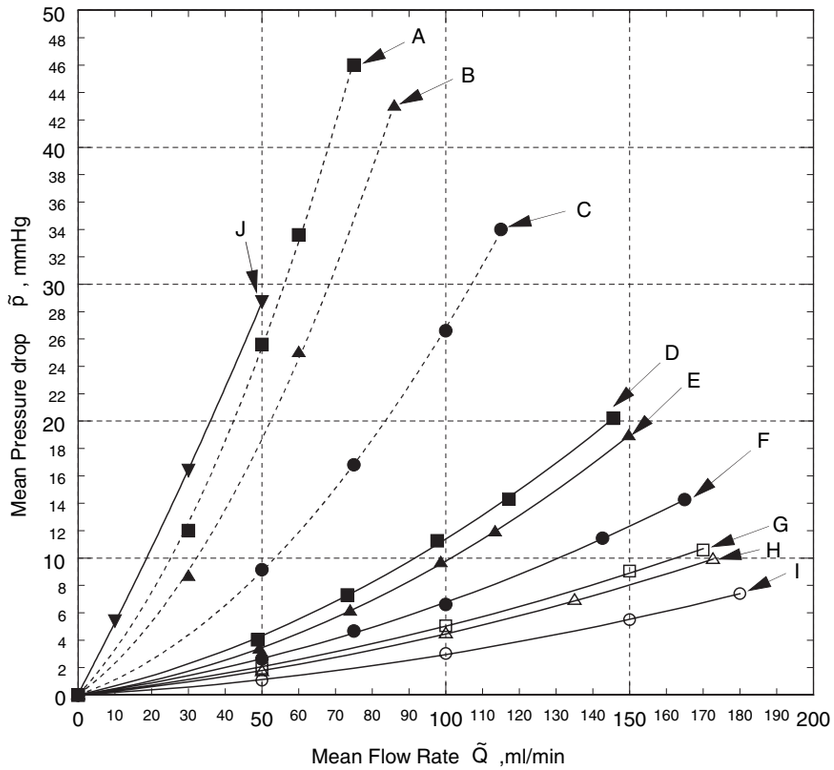

A: Pre-PTCA with 0.46 mm guidewire (27); **B**: Pre-PTCA with 0.35 mm guidewire (33); **C**: Pre-PTCA without guidewire (28); **D**: Intermediate with 0.46 mm guidewire (33); **E**: Intermediate with 0.35 mm guidewire (33); **F**: Intermediate without guidewire (33); **G**: Post-PTCA with 0.46 mm guidewire (30); **H**: Post-PTCA with 0.35 mm guidewire (33); **I**: Post-PTCA without guidewire (29); **J**: Post-PTCA with large angioplasty catheter (38).

Figure 8. Mean pressure drop ($\Delta\tilde{p}$) vs. mean flow rate ($\tilde{Q}$) in pre-PTCA, intermediate, and post-PTCA lesion with (0.35 and 0.46 mm) and without guidewire.

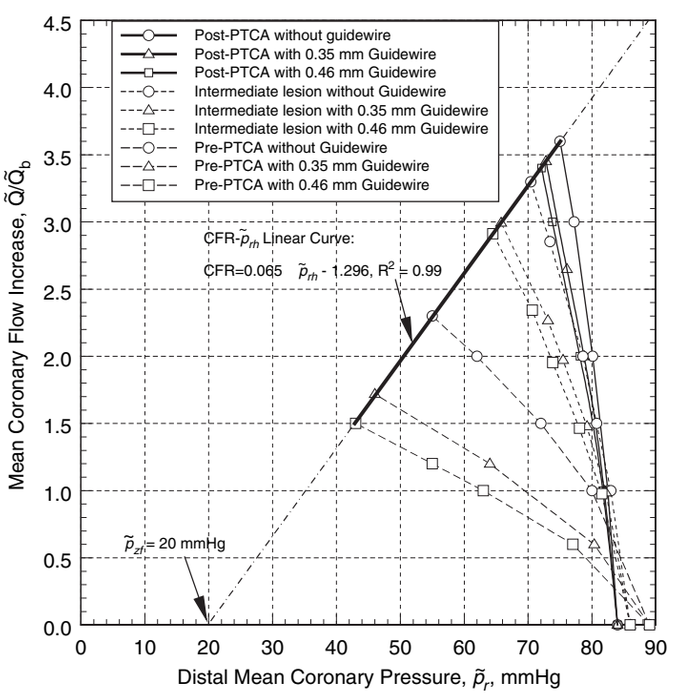

Figure 9. Relative mean coronary flow rate increase ($\tilde{Q}/\tilde{Q}_b$) vs. distal mean coronary $\tilde{p}_r$ before and after intervention. The maximum vasodilation-distal perfusion pressure relation ($CFR - \tilde{p}_{rh}$) is shown by the nearly linear solid line.

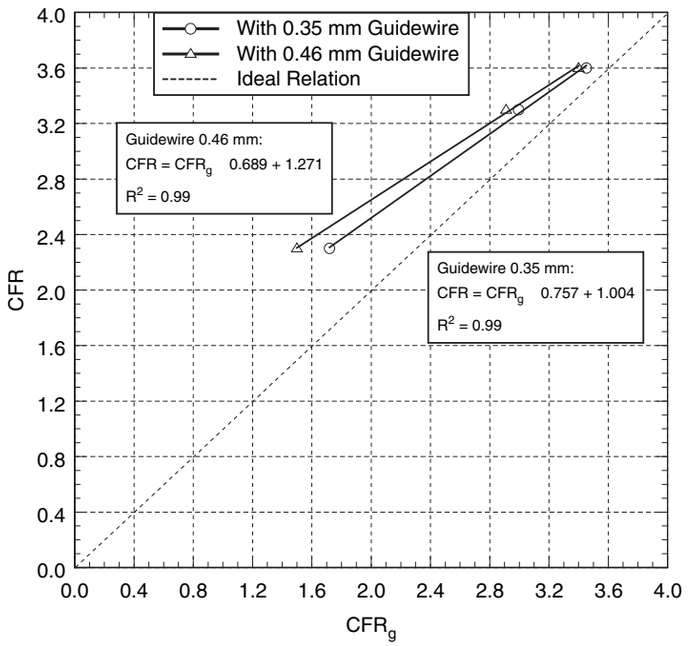

Figure 10. CFR vs. CFR_g correlation. Dotted line shows the ideal CFR vs. CFR_g relation.

($[d_i/d_m] = 0.48$) also indicated significant increases in flow resistance with the guidewire present (Tables 1 and 2). Similarly, the stenosis resistance $\tilde{R}_h$, defined as $(\Delta\tilde{p}_h/\tilde{Q}_h)$, decreased considerably from 0.30 mmHg/mL/min to 0.04 mmHg/mL/min from pre- to post-PTCA, respectively. With guidewire size 0.35 mm, $\tilde{R}_{h-g}$ decreased from 0.50 mmHg/mL/min for pre-PTCA to 0.06 mmHg/mL/min for post-PTCA. Although the 32 patient group (31) had a normal microvascular function, the presence of microvascular impairment could produce different correla-

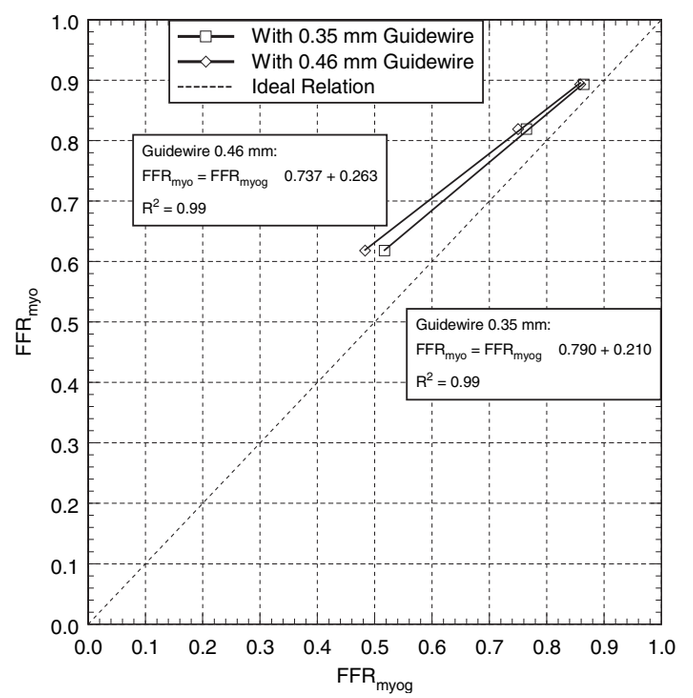

Figure 11. FFR_{myo} vs. $FFR_{myo\text{-}g}$ correlation (with $\tilde{p}_v \sim 0$). Dotted line shows the ideal FFR_{myo} vs. $FFR_{myo\text{-}g}$ relation.

tions between FFR_{myo}-FFR_{myog} and CFR-CFR_g with epicardial stenoses, and it could be the focus of future studies on guidewire effect and microcirculation, particularly moderately sized lesions (42).

Nomenclature

FFR_{myo} & $FFR_{myo\text{-}g}$ Myocardial fractional flow reserve without and with guidewire, respectively.

CFR & CFR_g Coronary flow reserve without and with guidewire, respectively.

$CFR_{doppler}$ Coronary flow reserve measured with Doppler guidewire.

CFR_{thermo} Coronary flow reserve measured with thermodilution technique.

$\tilde{Q}_h$ & $\tilde{Q}_{h-g}$ Coronary flow at hyperemia without and with guidewire, respectively.

$\tilde{Q}_b$ Coronary flow at basal condition without guidewire.

$\tilde{p}_{rh}$ & $\tilde{p}_{rh-g}$ Mean pressure distal to a stenosis without and with guidewire, respectively.

$\tilde{p}_a$ Mean aortic pressure.

$\tilde{p}_v$ Central venous pressure.

$\tilde{\mathrm{R}}\mathrm{e}$ Reynolds number $= \frac{4\tilde{Q}}{\pi\nu(1+\frac{d_i}{d_m})d_e}$

$rCFR_g$ Relative coronary flow reserve.

$\Delta\tilde{p}_h$ & $\Delta\tilde{p}_{h-g}$ Mean pressure drop without and with guidewire, respectively.

$\overline{u}_{p-t}$ Instantaneous velocity (mass averaged) at peak coronary flow.

$\tilde{\overline{u}}$ Time averaged mean coronary flow velocity (mass averaged).

$\overline{u}$ Instantaneous velocity (mass averaged).

η Dynamic blood viscosity.

η_∞ & η_0 Blood viscosity at infinte and zero shear rate, respectively.

λ Time constant.

ρ Blood density.

υ Kinematic blood viscosity.

$\tilde{p}_{zf}$ Zero coronary flow pressure.

$\tilde{R}_h$ & $\tilde{R}_{h-g}$ Stenosis resistance without and with guidewire, respectively.

1 mmHg = 0.133 kPa.

BIBLIOGRAPHY

1. Dotter CT, Judkins MP. Transluminal treatment of arteriosclerotic obstruction. Description of a new technic and a preliminary report of its application. 1964. Radiology 1989;172:904–920.
2. Baim DS. Percutaneous transluminal coronary angioplasty. Cardiac Catheterization, Angiography, and Intervention. 5th ed. Philadelphia, PA: Williams & Wilkins; 2000.
3. Dervan JP, McKay RG, Baim DS. The use of an exchange guide wire in coronary angioplasty. Cathet Cardiovasc Diagn 1985;11:207–212.
4. Pijls NH, De Bruyne B, Peels K, Van Der Voort PH, Bonnier HJ, Bartunek J, Koolen JJ. Measurement of fractional flow reserve to assess the functional severity of coronary-artery stenoses. N Engl J Med 1996;334:1703–1708.
5. Pijls NH, De Bruyne B, Smith L, Aarnoudse W, Barbato E, Bartunek J, Bech GJ, Van De Vosse F. Coronary thermodilution to assess flow reserve: validation in humans. Circulation 2002;105:2482–2486.
6. De Bruyne B, Pijls NH, Smith L, Wievegg M, Heyndrickx GR. Coronary thermodilution to assess flow reserve: experimental validation. Circulation 2001;104:2003–2006.
7. Siebes M, Verhoeff BJ, Meuwissen M, de Winter RJ, Spaan JA, Piek JJ. Single-wire pressure and flow velocity measurement to quantify coronary stenosis hemodynamics and effects of percutaneous interventions. Circulation 2004;109:756–762.
8. Ernst SM, Tjonjoegin RM, Schrader R, Kaltenbach M, Sigwart U, Sanborn TA, Plokker HW. Immediate sealing of arterial puncture sites after cardiac catheterization and coronary angioplasty using a biodegradable collagen plug: results of an international registry. J Am Coll Cardiol 1993;21:851–855.
9. Aker UT, Kensey KR, Heuser RR, Sandza JG, Kussmaul WG 3rd. Immediate arterial hemostasis after cardiac catheterization: initial experience with a new puncture closure device. Cathet Cardiovasc Diagn 1994;31:228–232.
10. Gruentzig AR, Senning A, Siegenthaler WE. Nonoperative dilation of coronary artery stenosis: Percutaneous transluminal coronary angioplasty. N Engl J Med 1979;301:61–68.
11. Ganz P, Harrington DP, Gaspar J, Barry WH. Phasic pressure gradients across coronary and renal artery stenoses in humans. Am Heart J 1983;106:1399–1406.
12. Ganz P, Abben R, Friedman PL, Garnic JD, Barry WH, Levin DC. Usefulness of transstenotic coronary pressure gradient measurements during diagnostic catheterization. Am J Cardiol 1985;55:910–914.
13. Anderson HV, Roubin GS, Leimgruber PP, Cox WR, Douglas JS Jr., King SB III, Gruentzig AR. Measurement of transstenotic pressure gradient during percutaneous transluminal coronary angioplasty. Circulation 1986;73:1223–1230.
14. Gould KL, Kirkeeide R, Buchi M. Coronary flow reserve as a physiologic measure of stenosis severity, part 1: Relative and absolute coronary flow reserve during changing aortic pressure and cardiac workload; part II: Determination from arteriographic stenosis dimensions under standardized conditions. J Am Coll Cardiol 1990;15:459–474.
15. Gould KL, Lipscomb K, Hamilton GW. Physiologic basis for assessing critical coronary stenosis: Instantaneous flow response and regional distribution during coronary hyperemia as measures of coronary flow reserve. Am J Cardiol 1974;33:87–94.
16. Gould KL. Coronary Artery Stenosis and Reversing Atherosclerosis. 2nd ed. London, UK: Arnold Publishers; 1999.
17. Pijls NHJ, De Bruyne B. Coronary pressure. 2nd ed. Amsterdam, The Netherlands: Kluwer Publishers; 1999.
18. Baumgart D, Haude M, Goerge G, Ge J, Vetter S, Dagres N, Heusch G, Erbel R. Improved assessment of coronary stenosis severity using the relative flow velocity reserve. Circulation 1998;98:40–46.
19. Pijls NH, Van Gelder B, Van der Voort P, Peels K, Bracke FA, Bonnier HJ, El Gamal MI. Fractional flow reserve: A useful

index to evaluate the influence of an epicardial coronary stenosis on myocardial blood flow. Circulation 1995;92:3183–3193.
20. De Bruyne B, Pijls NH, Bartunek J, Kulecki K, Bech JW, De Winter H, Van Crombrugge P, Heyndrickx GR, Wijns W. Fractional flow reserve in patients with prior myocardial infarction. Circulation 2001;104(2):157–162.
21. Meuwissen M, Siebes M, Chamuleau SA, Tijssen JG, Spaan JA, Piek JJ. Intracoronary pressure and flow velocity for hemodynamic evaluation of coronary stenoses. Expert Rev Cardiovasc Ther 2003;1:471–479.
22. Back LH. Estimated mean flow resistance increase during coronary artery catheterization. J Biomech 1994;27:169–175.
23. Kern MJ, Aguirre FV, Bach RG, Caracciolo EA, Donohue TJ. Translesional pressure – flow velocity assessment in patients: part I. Cathet Cardiovasc Diagn 1994;31:49–60.
24. Segal J, Kern MJ, Scott NA, King SB III, Doucette JW, Heuser RR, Ofili E, Siegel R. Alterations of phasic coronary artery flow velocity in humans during percautaneous coronary angioplasty. J Am Coll Cardiol 1992;20:276–286.
25. Doriot P, Dorsaz P, Dorsaz I, Chatelain P. Accuracy of coronary flow measurements performed by means of doppler wires. Ultra Med Biol 2000;26:221–228.
26. Wilson RF, Laxson DD. Caveat emptor: a clinician's guide to assessing the physiologic significance of arterial stenoses. Cathet Cardiovasc Diagn 1993;29:93–98.
27. Banerjee RK, Back LH, Back MR. Effects of diagnostic guidewire catheter presence on translesional hemodynamic measurements across significant coronary artery stenoses. Biorheology 2003;40(6):613–635.
28. Banerjee RK, Back LH, Back MR, Cho YI. Physiological flow analysis in significant human coronary artery stenoses. Biorheology 2003;40(4):451–476.
29. Banerjee RK, Back LH, Back MR, Cho YI. Physiological flow simulation in residual human stenoses after coronary angioplasty. ASME J Biomech Eng 2000;122:310–320.
30. Sinha Roy A, Back LH, Banerjee RK. Guidewire flow obstruction effect on pressure drop-flow relationship in moderate coronary artery stenosis. J Biomech 2006;39:853–64.
31. Wilson RF, Johnson MR, Marcus ML, Alyward PEG, Skorton DJ, Collins S, White CW. The effect of coronary angioplasty on coronary flow reserve. Circulation 1988;77:873–885.
32. Back LH, Denton TA. Some arterial wall shear stress estimates in coronary angioplasty. Adv Bioeng ASME BED 1992;22:337–340.
33. Sinha Roy A, Banerjee RK, Back LH, Back MR, Khoury SF, Millard RW. Delineating the guidewire flow obstruction effect in assessment of fractional flow reserve and coronary flow reserve measurements. Am J Physiol: Heart Circ Physiol 2005;289:H392–H397.
34. Cho YI, Back LH, Crawford DW, Cuffel RF. Experimental study of pulsatile and steady flow through a smooth tube and an atherosclerotic coronary artery casting of man. J Biomech 1983;16:933–946.
35. Cho YI, Kensey KR. Effects of non-Newtonian viscosity of blood on flows in a diseased arterial vessel: Part 1. Steady flows. Biorheology 1991;28:241–262.
36. Back LH, Radbill JR, Crawford DW. Analysis of pulsatile viscous blood flow through diseased coronary arteries of man. J Biomech 1977;10:339–353.
37. Womersley JR. Method for the calculation of velocity, rate of flow and viscous drag in arteries when the pressure gradient is known. J Physiol 1955;127:553–563.
38. Banerjee RK, Back LH, Back MR, Cho YI. Catheter obstruction effect on pulsatile flow rate-pressure drop during coronary angioplasty. ASME J Biomech Eng 1999;121:281–289.
39. Brown BG, Bolson EL, Dodge HT. Dynamic mechanisms in human coronary stenosis. Circulation 1984;170:917–922.
40. Bache RJ, Schwartz JS. Effect of perfusion pressure distal to a coronary stenosis on transmural myocardial blood flow. Circulation 1982;65:928–935.
41. De Bruyne B, Pijls NH, Paulus WJ, Vantrimpont PJ, Sys SU, Heyndrickx GR. Transstenotic coronary pressure gradient measurement in humans: In vitro and in vivo evaluation of a new pressure monitoring angioplasty guide wire. J Am Coll Cardiol 1993;22(1):119–126.
42. Fearon WF, Yeung AC. Evaluating intermediate coronary lesions in the cardiac catheterization laboratory. Rev Cardiovasc Med 2003;4:1–7.

See also Arteries, Elastic Properties of; Brachytherapy, Intravascular; Hemodynamics; Intraaortic Balloon Pump.